The subduction influence on ocean ridge basalts and its significance

Alexandra Yang Yang (yangyang@gig.ac.cn)
Guangzhou Institute of Geochemistry, Chinese Academy of Sciences https://orcid.org/0000-0002-5729-1588

Charles Langmuir
Harvard University

Yue Cai
Columbia University

Steven Goldstein
Columbia University

Peter Michael
University of Tulsa

Zhongxing Chen
Harvard University

Article

Keywords: mid-ocean ridge basalts, Arctic Gakkel Ridge, back-arc basins

Posted Date: January 8th, 2021

DOI: https://doi.org/10.21203/rs.3.rs-132754/v1

Version of Record: A version of this preprint was published at Nature Communications on August 6th, 2021. See the published version at https://doi.org/10.1038/s41467-021-25027-2.

Abstract

The plate tectonic cycle produces chemically distinct mid-ocean ridge basalts (MORB) and arc volcanics, with the latter enriched in fluid-mobile elements and depleted in Nb owing to fluxes from the subducted slab. Basalts from back-arc basins (BABB), with intermediate compositions, show that the subduction flux can escape the arc. Hence it is puzzling why arc signatures have rarely been recognized in MORB. Here we report the first MORB samples with distinct arc signatures, akin to BABB, from the Arctic Gakkel Ridge. A new high precision dataset for 576 Gakkel samples suggests a pervasive subduction influence. This influence can also be identified in Atlantic and Indian MORB with a “BABB filter”, but is nearly absent in Pacific MORB. This global distribution reflects the control of a “subduction shield” that has surrounded the Pacific Ocean for 180Myr. Statistics suggest that a flux equivalent to ~ 13% of output at arcs is incorporated into the convecting upper mantle.

Introduction

A long-standing paradigm of mantle geochemistry has been the clear distinction between mid-ocean ridge basalts (MORB) and convergent margin and continental rocks, with MORB having a small range of Ce/Pb and Nb/U ratios, around so-called “canonical values” of 25 and 47[1–5] (Fig. 1a), in contrast to arcs where both ratios are generally less than 5[6]. An inference from such observations would be that the subduction flux that dominates arc magmatic chemistry contributes minimally to the convecting upper mantle, and that arc and rear arc volcanism effectively extracts the subduction flux. Indeed, with important exceptions[7–10], a subduction flux seems largely to be absent in MORB.

There are, however, prominent exceptions. The most common are the spreading centers in back-arc basins, which erupt back-arc basin basalt (BABB) that are intermediate in composition between MORB and arc volcanics. In front of the arc, an exception is the southern Chile Ridge, where a “slab window” permits subduction-modified mantle wedge material to flow under the neighboring spreading center[7]. We know from BABB in particular that not all the subduction flux is captured by the arc. But most arcs do not have back-arc basins. Where back-arc basins are not present, should not the subduction-modified mantle that would be sampled if there were a back-arc basin contribute a component to the convecting asthenosphere? And in this case should it not then occasionally reappear and be sampled at ocean ridges? To explore these questions requires a careful examination of MORB data to see if a signal akin to BABB might be more widespread than the few existing occurrences where it has been inferred[7–10].

A key to look for this component would be in element ratios such as Ce/Pb and Nb/U that are akin to BABB, with a modest arc signature. The MORB dataset does in fact contain large variations in these ratios both regionally and globally[5,11] (Supplementary Information), and even the compiled global MORB data set of Gale, et al.[12] has Nb/U of 25 to 75 and Ce/Pb from 10 to > 100 (Fig. 1a). Analytical problems for Ce/Pb and Nb/U ratios in MORB historically have been severe, however, resulting from Pb contamination, alteration effects on U, and large uncertainties at low U and Pb concentrations (Supplementary Information). There is a cluster around the canonical values that is completely distinct

from arc basalts, with BABB having intermediate values (Fig. 1a), but the possibility of recognizing an important signal *within* the MORB data is obscured by the various difficulties.

A Subduction Signal On The Gakkel Ridge

Laser ablation analysis of glass chips avoids the problems of alteration (U) and contamination (Pb), and permits far larger datasets than can be acquired by laborious solution techniques. To this end, we have developed precise and accurate laser ablation methods, and reanalyzed major and trace elements on the complete set of 576 previously analyzed Gakkel MORB glasses from 130 dredge stations[12-14] (Supplementary Tables 1 and 3). We unexpectedly discovered arc-like trace element characteristics (Fig. 1) in multiple samples from two dredges, which we confirmed by resampling the dredges to analyze further samples. The most extreme samples have low Nb/U (8-10) and Ce/Pb (7-8), akin to samples from back-arc basins (Fig. 1a), with distinct negative Nb-Ta and positive Pb anomalies (Fig. 1c). The samples also have higher H_2O/Ce (261-415) than average global MORB (~200[15,16]), higher $^{207}Pb/^{204}Pb$ and $^{208}Pb/^{204}Pb$ ratios relative to the northern hemisphere reference line, higher $^{87}Sr/^{86}Sr$ (up to 0.7037) and low $^{143}Nd/^{144}Nd$ ratios (~0.5128) (Supplementary Table S1).

These data raise the question whether there might be a more pervasive subduction influence in this region. Indeed, the positive correlation between Nb/U and Ce/Pb ratios from the new laser data suggests a subduction influence on the Gakkel MORB (Fig. 1b), which is observed in elevated Th/Nb and K_2O/TiO_2 ratios relative to $(La/Sm)_N$ ratios as well (Supplementary Fig. S3). The Gakkel MORB also have a significant water enrichment compared to other MORB globally, with an average H_2O/Ce of 275±51, compared to 206±48 for Pacific MORB (average from our data compilation). High H_2O/Ce ratios coupled with arc-like Nb/U and Ce/Pb ratios support subduction contributions to the Gakkel mantle. Then, where did the H_2O -rich material come from?

Although no proximal subduction zone is present to provide slab-derived materials, the Arctic has been surrounded by subduction zones at least during the past 200 Myr, for example, Mogol-Okhotsk Plate from 200-160 Ma, Farallon Plate from 200-100 Ma, South Anuyi Plate from ~140 to 160 Ma and Izanagi Plate from 100 to 40 Ma[17,18](Fig. 2a and Supplementary Fig. S4). It appears a portion of the subduction flux was incorporated in the mantle wedge corner flow and escaped the arc. Some of this modified mantle would then contribute to the asthenosphere that was later sampled by spreading when the Gakkel ridge began to spread. Plate reconstruction suggests that these past subduction zones, likely metasomatized sub-arc mantle, were located right beneath or near the current spreading Gakkel ridge (Fig. 2a). Such a mechanism would provide a subduction flux to the Arctic mantle to contribute to the current MOR magmatism (Fig. 2a and Supplementary Fig. S4).

Identifying Subduction Signals In Global Morb Using A “babb Filter”

The observation of a subduction influence on the Gakkel Ridge leads to expectations of a more widespread effect. Plates in the Pacific Ocean have had long subduction histories beneath the Eurasian and American plates as well as the Arctic (Fig. 2), leading to the possibility that subduction signals could be present in the Indian and Atlantic Oceans. In contrast, the lack of subduction feeding the sub-Pacific mantle leads to the expectation of no subduction signal for Pacific ridges.

We update here the global data base of Gale, et al. [12], with recently published high-quality data (Supplementary Table S6). The final data set adds ~ 3000 new analyses to the Gale compilation (not including the new Gakkel data) that can be used to evaluate the subduction signal on a global basis.

The appropriate comparison for the signal that escapes the arc is not the arc front itself, but the BABB that we know reflect a subduction signal that emerges beyond the arc. To cope with potential problems with literature Pb and U data, additional ratios sensitive to subduction such as Ba/Nb and Rb/Nb are needed. Over 94% of global BABB have Ba/Nb>6 and Rb/Nb>0.6, and over 92% of them have Nb/U<42 and Ce/Pb<22 (Fig. 3). Therefore, these four ratios can be used to construct a “BABB filter” such that if at least three of the four ratios meet the BABB criteria, the sample has a subduction influence. Using any 3 instead of all four leaves some room for analytical error, in case a real BABB-like MORB has a bad Pb, or U measurement. This filter provides a simple true or false test for subduction influence. The efficacy of the BABB filter is good: 94% of global BABB data, yet only 2% of Pacific MORB (apart from the southern Chile Ridge) pass the filter. For the Gakkel Ridge, 229 of 710 samples pass the filter, showing a pervasive subduction influence.

For the global ocean ridge system, of the 4945 samples with at least three of the ratios available to use the BABB filter, 681 samples pass the filter, leading to the conclusion that 14 percent of global MORB, and over 19% of MORB outside the Pacific basin, contain an observable subduction influence.

Compared with Pacific MORB, BABB-like MORB show enrichments not only in Rb, Ba, U, and Pb (elements included in the BABB filter), but also show clear peaks in Cs, K and Th (Fig. 4a). All these elements are enriched in arc volcanics relative to Pacific MORB, supporting that the main differences of BABB-like MORB relative to Pacific MORB are caused by subduction input. Such conclusions can also be tested using water contents and Sr isotopes in MORB. Global BABB have much higher H_2O/Ce ratios due to the contribution of slab-derived volatiles in their source[19,20], along with an offset to higher $^{87}Sr/^{86}Sr$ ratios relative to $^{143}Nd/^{144}Nd$ ratios compared to Pacific MORB (Fig. 4 b-d). Global BABB-like MORB have higher H_2O/Ce ratios of 293±75 (1SD) compared to those from Pacific MORB (205±49, 1SD), consistent with a slightly hydrated mantle source with BABB signatures. The BABB-like MORB also shift towards higher $^{87}Sr/^{86}Sr$ ratios for given $^{143}Nd/^{144}Nd$ ratios compared to Pacific MORB, plotting mostly within the BABB field.

Since both convergent margins and continental crust have extreme values of the ratios used for the BABB filter, the question arises if one can distinguish whether the observations presented here might be caused by addition of continental components. A notable feature of many of the subduction-infuenced MORB is

that they are neither enriched in the rare earth ratio La/Sm nor do they have exceptionally low Nd isotopes compared to Pacific MORB (Fig. 4 d,e). Upper continental crustal components have elevated $(La/Sm)_N$ (up to 4[21]) and low Nd isotopes[22], and do not succeed as a main source component for the majority (>60%) of BABB-like MORB with $(La/Sm)_N$ <1, and $^{143}Nd/^{144}Nd$ higher than 0.513 (Fig. 4 d,e). More importantly, continental crust is dry with H_2O/Ce of ~ 120 for upper crust and ~50 for the lower crust (calculation on H_2O/Ce of continental crust can be found in the Methods section), which could not account for the hydrous feature of BABB-like MORB.

Quantitative Assessment On The Subduction Flux In The Source Of Global Morb

To quantify the relative contributions of subduction input in the global MORB, we assume Nb in the source of BABB-like MORB receives minimal contribution from the subducted slab, and the subduction flux can be calculated by the relative enrichment of fluid-mobile elements (e.g., Cs, Rb, Ba Th, U, and K) which are known to be contributed by slab-derived fluids/melts[23] (Fig. 4a) over Nb. The ambient mantle without subduction influence is assumed to have the Cs/Nb, Rb/Nb, Ba/Nb, U/Nb, Th/Nb and K/Nb ratios of average Pacific MORB, and these ratios would not change greatly during mantle melting for MORB and arc magma genesis as they are all highly incompatible elements. Therefore, the subduction flux (f) for each element in BABB-like MORB ($f^{\text{B-MORB}}$), Rb, for example, then could be estimated by the average Rb concentrations in BABB-like MORB multiplied by the total melt volume of BABB-like MORB, minus the ambient mantle Rb contributions before subduction input which can be estimated by Nb concentrations and Rb/Nb ratios of ambient mantle (AM).

$$f_{\text{Rb}}^{\text{B-MORB}} = (\text{Rb}_{\text{B-MORB}} - \text{Nb}_{\text{B-MORB}} \times \text{Rb/Nb}_{\text{AM}}) \times \text{melt volume}_{\text{B-MORB}}$$

$$f_{\text{Rb}}^{\text{arc}} = (\text{Rb}_{\text{arc}} - \text{Nb}_{\text{arc}} \times \text{Rb/Nb}_{\text{AM}}) \times \text{melt volume}_{\text{arc}}$$

Melt production at global ocean ridges has been estimated to be 21 km^3/yr[24], and the melt volume of BABB-like MORB which make up 14% of global ocean ridge production, are ~2.94 km^3/yr. The melt volume at global arcs is estimated to be ~3 km^3/yr, calculated with the average arc magmatic addition rate of $60km^3/Ma/km$[25], along with the ~50,000km length of global arcs[26]. Average compositions of Pacific MORB, BABB-like MORB and arc volcanics can be found in Table S5.

This equation can then be used to estimate the subduction flux of Cs, Ba, U, Th and K erupted in BABB-like MORB and in arc volcanics, to arrive at a minimum estimate of the subduction flux that escapes the convergent margin to be incorporated into upper mantle flow. What proportion of the subduction flux would need to make it into the convecting mantle to produce the signal observed in MORB? The portion of subduction flux beneath MORB compared to arc can be calculated by $f^{\text{B-MORB}}/f^{\text{arc}}$ for each element. The result

shows that a flux equivalent to ~13% of the erupted flux at convergent margins is disseminated in MORB (Table 1).

	Cs	Rb	Ba	U	Th	K	average
$f^{B\text{-}MORB}/f^{arc}$	11%	19%	12%	8%	18%	9%	13%

Table 1. Estimated subduction fluxes for Cs, Rb, Ba, U, Th, and K in MORB relative to the global output at arcs. Subduction flux averaged for all the elements are listed in the last column.

Based on the widely held idea that Nb/U and Ce/Pb of oceanic basalts show only small deviations from the “canonical values”, it has seemed that subduction fluxes rarely appear at ridges, or that the influence has been globally uniform[1]. The new data presented here suggest instead that a small but significant fraction of the subduction flux can be widely and heterogeneously disseminated in the shallow asthenospheric mantle.

Geographical Pattern Of The Subduction Influence And The Pacific Subduction Shield

The subduction influence shows clearly defined regional variations. The subduction influence is present in only 2% of Pacific MORB, 12% for the Atlantic as a whole, 26% for the Indian and 32% for Gakkel MORB. Along the MAR, there are also clear provinces. A large region in the equatorial Atlantic between 33°N and 34°S has less than 3% of samples passing the BABB filter, similar to the Pacific. Where the Chile Ridge is being subducted beneath South America, opening a slab window into the arc-influenced mantle wedge[27], there is a clear BABB signal. These spatial regularities can then be mapped into regions that have less than 3% and those that have more than 20% BABB-like MORB (Fig. 5a). The former is Pacific-like with minimal subduction input, and the latter can be considered to receive considerable amount of subduction flux.

What is striking is the lack of subduction influence apart from the Chile Ridge in the Pacific Ocean. If the cause of the observations presented here is indeed subduction, the lack of subduction influence in the Pacific can be understood from global tectonic reconstructions which show that around the Pacific Ocean there has been a continuous “subduction shield” for at least the last 180 million years[17]. This subduction shield would strictly limit the contribution of the subduction component to sub-Pacific mantle, simply explaining the striking absence of this component in Pacific MORB today. In this case, older Pacific basalts should also have no subduction influence, which is supported by the glasses from the oldest Pacific crust drilled at Holes 801 and 1149[28], of which none of the ratios pass the BABB filter (Fig.

5a). Further support comes from the older samples outside the subduction shield in the western Pacific, where BABB-influenced samples are pervasive (Fig. 5a).

Interestingly, the equatorial Atlantic between 33°N and 34°S, as well as the easternmost Indian Ocean have Pacific-like signatures, with less than 3% of samples passing the BABB filter (Fig. 5a). Such an observation provides additional evidence for the outflow of Pacific mantle as a consequence of shrinking Pacific Ocean[29]. The Caribbean and the Southeast Indian Ocean are thus likely gateways for Pacific mantle outflow, whereas the Drake passage, with strong subduction signals (Fig. 5a), might not be such a gateway. Such an inference is consistent with previous study based on Pb isotopes[30].

It is noteworthy that BABB-influenced mantle occupies similar geographical regions as the “Dupal” isotopic anomaly, which was identified in the Atlantic and Indian Oceans with elevated $^{208}Pb/^{204}Pb$ (and $^{207}Pb/^{204}Pb$) for given $^{206}Pb/^{204}Pb$ ratios[13,31,32]. The influence we have identified, however, is distinct from Dupal. Sixty-one percent of global MORB samples with a Dupal isotopic signature of $\triangle 8/4$ (elevated $^{208}Pb/^{204}Pb$ to $^{206}Pb/^{204}Pb$) >30[13,32] do not pass the subduction filter. The eastern part of the Southeast Indian Ridge, for example, has a strong Dupal signature but no BABB-influenced samples (Fig. 5a and Supplementary Fig. S6-7). More importantly, MORB with extreme Dupal signature ($\triangle 8/4$~100) are dry with Pacific-like H_2O/Ce ratios (<200), and those with lower $\triangle 8/4$ tend to have higher H_2O/Ce ratios (Supplementary Fig. S5). Such a negative correlation for Dupal and subduction input for global BABB-like MORB suggests a dilution effect on the Dupal signature by recent subduction flux. These observations indicate that recent subduction is not the cause of the global distribution of the Dupal anomaly, but instead superimposes a subduction influence on the pre-existing large-scale mantle heterogeneity, of whatever flavor it may be. Both the Dupal and the BABB-influenced regions are located where subduction and ancient continental break-up occurred, outside the current subduction shield. The subduction shield may thus also be relevant for the location of the Dupal region, and the isolation of Pacific mantle caused by subduction shields may be much longer than the past 180 Myr, which might be traced back to 400 Ma when Paleo-Pacific Ocean started to subduct beneath the Gondwana supercontinent[33].

Subduction is a global process and the subduction influence in the back-arc basins beyond the volcanic fronts of convergent margins has long been known. This influence must reside in the upper mantle, and upon reflection, it has been mysterious that this influence has been so rarely described in ocean ridge basalts. The observations presented here demonstrate that there is indeed a widespread subduction influence on MORB, manifested clearly in 19% of global MORB samples outside of the Pacific Ocean basin. The geographical distribution of this influence can be understood in the context of the long-term tectonic history of plate movements and the global distribution of subduction zones.

Methods

Trace elements

The major and trace elements were measured using a RESOlution-S155 193nm Excimer laser connected to a Thermo iCAP Q ICP-MS which is used only for laser ablation analyses at Harvard University. Two points per chip were obtained, and the values reported are the average of the two analyses. Ca contents of the major element analysis of the same chip were used as an internal standard. Data were then reduced using basalt standard BHVO-2G run in the same run (values in Table S2), which was also used as a drift correction standard run every ten analyses. The Harvard lab basalt glass standard VE32 was present in every probe mount, and was analyzed as an unknown with the other samples to get estimates of between run reproducibility over the course of this study. VE32 data were very consistent between runs (Table S2), and provide good estimates of the errors in the analyses, which generally scale with concentration (Table S2).

Water

Concentrations of H_2O dissolved in glasses were analyzed by Fourier Transform Infrared Spectroscopy (FTIR) at the University of Tulsa using published methods and calibrations[43,44] with slight modifications[15]. Doubly polished glass wafers, 100-250μm thick, were placed atop a 2mm thick KBr pellet and analyzed using a NicPlan IR microscope equipped with a HgCdTe detector, attached to a Nicolet 520 FTIR. Thickness was measured by two methods: firstly by digital micrometer, and secondly by focusing the calibrated z-axis of the FTIR microscope stage on the glass wafer and on the adjacent KBr disk using reflected light. Optically clear areas of known thickness (± 2μm), 80 x 80 μm, were analyzed with 256 scans/spot. Absorbance at the broad 3550 cm^{-1} (combined OH and H_2O) and 1630 cm^{-1} (molecular H_2O only) peaks were measured after subtraction of interpolated backgrounds. Density was assumed to be 2.8 g/cm^3. Molar absorption coefficients used for all glasses were: 63 l/mol-cm for 3550 and 25 l/mol-cm for e1630. Analyses are the average of 3-4 spot determinations of 3550 cm^{-1} on two separate wafers. Replicate analyses of different wafers from the same specimen were typically reproducible to ±5%.

Sr-Nd-Pb isotopes

Column chromatographic procedures for Sr-Nd-Pb purifications were carried out in Class 100 or Class 1000 ultra-clean chemistry lab at Lamont-Doherty Earth Observatory following routine procedures[45]. Hand-selected clean glass chips were sonicated in cold 8N HNO_3 in the sonicator for 10 minutes and washed with quartz-distilled water 4 times prior to standard HNO_3-HF hotplate digestions. Pb was extracted using BioRad® AG1-X8 resin. Sr was extracted using Eichrom Sr resin. Rare Earth Elements (REE) were extracted using Tru-Spec® resin. Nd was extracted from the REE cut either using alpha-hydroxyisobutyric acid (alpha-HIBA) and BioRad® AG50-X8 resin or using Eichrom® Ln resin and 0.22 N HNO_3 acid.

Isotopes were measured on a VG-Axiom multicollector-inductively coupled mass spectrometer (MC-ICPMS). In-run mass fractionations are normalized using $^{86}Sr/^{88}Sr = 0.1194$, and $^{146}Nd/^{144}Nd = 0.7219$.

All samples were further normalized to the $^{86}Sr/^{88}Sr$ value of 0.71024 for SRM 987, $^{143}Nd/^{144}Nd$ value of 0.511858 for La Jolla, and $^{206}Pb/^{204}Pb$, $^{207}Pb/^{204}Pb$ and $^{208}Pb/^{204}Pb$ values of 16.9356, 15.4891, and 36.7006 for NBS 981[46], respectively.

Pb total procedure blank is always below 100 pg. As procedural blanks are negligible given the sample size and current analytical uncertainties, no blank corrections were performed. Measurements of international standard sample BCR-2 (after acid leach) yielded 0.704998 ±0.000013 (2σ, n=6) for $^{87}Sr/^{86}Sr$, 0.512609 ± 0.000006 (2σ, n=3) for $^{143}Nd/^{144}Nd$, as well as 18.7895±0.0008, 15.6523±0.0007, and 38.8845±0.0019 (2σ, n=1) for $^{206}Pb/^{204}Pb$, $^{207}Pb/^{204}Pb$, $^{208}Pb/^{204}Pb$ ratios, respectively, which is consistent with the published values of Weis et al.[47]: $^{87}Sr/^{86}Sr$ = 0.705019 ±0.000016 (2σ, n=13), $^{143}Nd/^{144}Nd$ = 0.512634 ±0.000012 (2σ, n=11), $^{206}Pb/^{204}Pb$ =18.8000±0.0020, $^{207}Pb/^{204}Pb$ =15.6236±0.0016, and $^{208}Pb/^{204}Pb$ = 38.8244±0.0034 (2σ, n=2).

The advantage of using Rb/Nb, Ba/Nb, Nb/U, and Ce/Pb to construct the BABB filter

Rb, Ba, Nb, and U as well as Ce and Pb are known to have similar incompatibility during magmatic processes, respectively, thus these element pairs would not be significantly fractionated from each other and these ratios should reflect source characteristics. There are, however, complicating factors. Alteration increases Rb and U contents[28] relative to Nb, contamination increases Pb relative to Ce, and mantle metasomatism by very low degree melt would increase Rb and Ba over Nb. Thus, various geological processes would lead to variations in each of the four ratios that would not be caused by subduction influence. Using any three of these four ratios to pass the filter minimizes the possibility of alteration, contamination and source enrichment effect leading to a spurious conclusion with respect subduction influence, and also means that a single anomalous ratio does not rule out that influence. Also, in case a real BABB-like MORB has a bad Pb, or U measurement, using any 3 instead of all four leaves some room for analytical error.

Global BABB-like MORB: additional evidence from H_2O/Ce and $^{87}Sr/^{86}Sr$ vs. $^{143}Nd/^{144}Nd$

Enrichments of Rb, Ba, Th, U and Pb in oceanic basalts have been proposed to result from continental crust materials mixed in the convecting mantle[48], thus, it is important to distinguish the subduction contribution versus continental crust additions in the source of BABB-like MORB. H_2O/Ce ratios are particularly useful as dehydration of the subducted slab would undoubtedly enrich the sub-arc wedge in H_2O relative to Ce[15], leading to much higher H_2O/Ce ratios for rocks with subduction contributions than Pacific MORB average (~200[15,16]). The continental crust, on the other hand, is dry. The upper continental crust can contain up to 8000 ppm water, mainly in hydrous minerals or as fluid inclusions in felsic minerals such as quartz and feldspars[49] and lower continental crust is estimated to contain water of less than 1000 ppm according to studies of granulite xenoliths[50]. The H_2O/Ce ratios, which could then be calculated with average Ce contents of continental crust[21], are 127 for upper continental crust, and 50 for

lower continental crust. Therefore, contribution of continental crust materials would result in lower H_2O/Ce ratios, contrary to the subduction contributions.

Data on water concentrations are far more limited than data for ICP-MS elements. BABB-like MORB, however, have higher H_2O/Ce ratios than the Pacific samples without subduction influence (Fig. 3b,c). Michael[15] and Dixon, et al.[16] noted that higher H_2O/Ce ratios in the North Atlantic might be related to a subduction signature. The higher average H_2O/Ce ratios for global BABB-like MORB, along with higher Ba/Nb, Rb/Nb and Th/Nb (Fig. 3), as well as lower Nb/U and Ce/Pb ratios, suggesting the Ba, Rb, Th, U, and Pb enrichments in BABB-like MORB mainly result from subduction input, rather than continental crust additions.

Continental crust addition would also lead to higher $^{87}Sr/^{86}Sr$ coupled with lower $^{143}Nd/^{144}Nd$ ratios for the derived basalts[48] and higher La/Sm ratios. Yet, we observe a shift to higher $^{87}Sr/^{86}Sr$ with limited variations in $^{143}Nd/^{144}Nd$ and $(La/Sm)_N$ ratios for most BABB-like MORB relative to Pacific MORB (Fig. 3d,e). Pacific MORB can then be used to set up a reference line (PMRL) to calculate the deviation of $^{87}Sr/^{86}Sr$ relative to $^{143}Nd/^{144}Nd$ ratios: δSr.

$$\delta Sr=(\,^{87}Sr/^{86}Sr\text{-}2.0492+2.6244\times\,^{143}Nd/^{144}Nd)\times 10^4$$

BABB-like MORB show good correlations of δSr with Ba/Nb, Rb/Nb, Ce/Pb, Th/Nb and H_2O/Ce ratios, trending towards BABB field (Fig S8), indicating greater mobility of Sr in slab derived fluids than Nd[51]. Additionally, the majority (60%) of BABB-like MORB are depleted N-MORB with $(La/Sm)_N<1$ (Fig. 3e), also indicating continent crust did not play an important role in the source of BABB-like MORB. All these observations are consistent with a subduction influence for these samples.

It is important to note, however, that the effect of subduction-induced enrichment in fluid-mobile elements (FME: Cs, Rb, Ba, Th, U, Pb and K) and Sr isotopic variations may vary with the original heterogeneity of ambient mantle. When the ambient mantle is rather depleted (high $^{143}Nd/^{144}Nd$ ratios comparable with Pacific MORB), subduction influence can cause considerable shifts towards higher $^{87}Sr/^{86}Sr$ ratios as shown by global BABB samples and BABB-like MORB. But as the ambient mantle becomes more enriched, the BABB enrichment will have less effect on the Sr isotopes and FME because enriched ambient mantle would have higher Sr and FME contents (Fig. 3d).

References

1. Chauvel, C., Goldstein, S. L. & Hofmann, A. W. Hydration and dehydration of ocean crust controls Pb evolution in the mantle. *Chem. Geol.* **126**, 65–75, doi:10.1016/0009-2541(95)00103-3 (1995).
2. Hofmann, A. W. Mantle geochemistry: The message from oceanic volcanism. *Nature* **385**, 219–229, doi:10.1038/385219a0 (1997).

3. Hofmann, A. W., Class, C. & Goldstein, S. L. Size and composition of the residual and depleted mantle reservoir. *Preprint at* https://www.essoar.org/doi/pdf/10.1002/essoar.10501102.*1*, 43, doi:doi:10.1002/essoar.10501102.1 (2020).
4. Hofmann, A. W., Jochum, K., Seufert, M. & White, W. M. Nb and Pb in oceanic basalts: new constraints on mantle evolution. *Earth Planet. Sci. Lett.* **79**, 33–45 (1986).
5. Sun, W. *et al.* Constancy of Nb/U in the mantle revisited. *Geochim. Cosmochim. Acta* **72**, 3542–3549, doi:10.1016/j.gca.2008.04.029 (2008).
6. Turner, S. J. & Langmuir, C. H. The global chemical systematics of arc front stratovolcanoes: Evaluating the role of crustal processes. *Earth Planet. Sci. Lett.* **422**, 182–193, doi:10.1016/j.epsl.2015.03.056 (2015).
7. Klein, E. M. & Karsten, J. L. Ocean-ridge basalts with convergent-margin geochemical affinities from the Chile Ridge. *Nature* **374**, 52 (1995).
8. le Roux, P. J. *et al.* Mantle heterogeneity beneath the southern Mid-Atlantic Ridge: trace element evidence for contamination of ambient asthenospheric mantle. *Earth Planet. Sci. Lett.* **203**, 479–498, doi:Pii s0012-821 × (02)00832-410.1016/s0012-821 × (02)00832-4 (2002).
9. Rehkämper, M. & Hofmann, A. W. Recycled ocean crust and sediment in Indian Ocean MORB. *Earth Planet. Sci. Lett.* **147**, 93–106, doi:10.1016/s0012-821x(97)00009-5 (1997).
10. Janney, P. E., Le Roex, A. P. & Carlson, R. W. Hafnium isotope and trace element constraints on the nature of mantle heterogeneity beneath the central Southwest Indian Ridge (13°E to 47° E). *J. Petrol.* **46**, 2427–2464, doi:10.1093/petrology/egi060 (2005).
11. Sims, K. W. W. & DePaolo, D. J. Inferences about mantle magma sources from incompatible element concentration ratios in oceanic basalts. *Geochim. Cosmochim. Acta* **61**, 765–784, doi:10.1016/s0016-7037(96)00372-9 (1997).
12. Gale, A., Dalton, C. A., Langmuir, C. H., Su, Y. & Schilling, J.-G. The mean composition of ocean ridge basalts. *Geochem. Geophys. Geosyst.* **14**, 489–518, doi:10.1029/2012GC004334 (2013).
13. Goldstein, S. L. *et al.* Origin of a 'Southern Hemisphere'geochemical signature in the Arctic upper mantle. *Nature* **453**, 89–93 (2008).
14. Michael, P. *et al.* Magmatic and amagmatic seafloor generation at the ultraslow-spreading Gakkel ridge, Arctic Ocean. *Nature* **423**, 956–961 (2003).
15. Michael, P. Regionally distinctive sources of depleted MORB: Evidence from trace elements and H2O. *Earth Planet. Sci. Lett.* **131**, 301–320, doi:10.1016/0012-821x(95)00023-6 (1995).
16. Dixon, J. E. *et al.* Light Stable Isotopic Compositions of Enriched Mantle Sources: Resolving the Dehydration Paradox. *Geochemistry Geophysics Geosystems* **18**, 3801–3839, doi:10.1002/2016gc006743 (2017).
17. Seton, M. *et al.* Global continental and ocean basin reconstructions since 200 Ma. *Earth-Science Reviews* **113**, 212–270, doi:10.1016/j.earscirev.2012.03.002 (2012).

18. Shephard, G. E., Müller, R. D. & Seton, M. The tectonic evolution of the Arctic since Pangea breakup: Integrating constraints from surface geology and geophysics with mantle structure. *Earth-Science Reviews* **124**, 148–183 (2013).
19. Stolper, E. & Newman, S. The role of water in the petrogenesis of Mariana Trough magmas. *Earth Planet. Sci. Lett.* **121**, 293–325, doi:10.1016/0012-821x(94)90074-4 (1994).
20. Bezos, A., Escrig, S., Langmuir, C. H., Michael, P. J. & Asimow, P. D. Origins of chemical diversity of back-arc basin basalts: A segment-scale study of the Eastern Lau Spreading Center. *Journal of Geophysical Research-Solid Earth* **114**, doi:10.1029/2008jb005924 (2009).
21. Rudnick, R. & Gao, S. Composition of the continental crust. *Treatise on Geochemistry* **3**, 1–64 (2003).
22. Plank, T. The chemical composition of subducting sediments. *Treatise on Geochemistry* (2014).
23. Pearce, J. A., Stern, R. J., Bloomer, S. H. & Fryer, P. Geochemical mapping of the Mariana arc-basin system: Implications for the nature and distribution of subduction components. *Geochemistry Geophysics Geosystems* **6**, doi:10.1029/2004gc000895 (2005).
24. Crisp, J. A. Rates of magma emplacement and volcanic output. *J. Volcanol. Geotherm. Res.* **20**, 177–211, doi:10.1016/0377-0273(84)90039-8 (1984).
25. Dimalanta, C., Taira, A., Yumul, G. P., Tokuyama, H. & Mochizuki, K. New rates of western Pacific island arc magmatism from seismic and gravity data. *Earth Planet. Sci. Lett.* **202**, 105–115, doi:10.1016/s0012-821x(02)00761-6 (2002).
26. Bird, P. An updated digital model of plate boundaries. *Geochemistry Geophysics Geosystems* **4**, doi:10.1029/2001gc000252 (2003).
27. Russo, R. *et al.* Subduction of the Chile Ridge: Upper mantle structure and flow. *Gsa Today* **20**, 4–10 (2010).
28. Kelley, K. A., Plank, T., Ludden, J. & Staudigel, H. Composition of altered oceanic crust at ODP Sites 801 and 1149. *Geochemistry Geophysics Geosystems* **4**, doi:891010.1029/2002gc000435 (2003).
29. Alvarez, W. Geological evidence for the geographical pattern of mantle return flow and the driving mechanism of plate tectonics. *Journal of Geophysical Research: Solid Earth* **87**, 6697–6710 (1982).
30. Pearce, J. A., Leat, P., Barker, P. & Millar, I. Geochemical tracing of Pacific-to-Atlantic upper-mantle flow through the Drake Passage. *Nature* **410**, 457–461 (2001).
31. Dupré, B. & Allègre, C. J. Pb-Sr isotope variation in Indian Ocean basalts and mixing phenomena. *Nature* **303**, 142–146 (1983).
32. Hart, S. R. A large-scale isotope anomaly in the Southern Hemisphere mantle. *Nature* **309**, 753–757 (1984).
33. Doucet, L. S. *et al.* Distinct formation history for deep-mantle domains reflected in geochemical differences. *Nat. Geosci.* **13**, 511–515 (2020).
34. McDonough, W. F. & Sun, S. S. The composition of the Earth. *Chem. Geol.* **120**, 223–253 (1995).
35. Young, A. *et al.* Global kinematics of tectonic plates and subduction zones since the late Paleozoic Era. *Geoscience Frontiers* **10**, 989–1013 (2019).

36. Shimizu, K. *et al.* Identifying volatile mantle trend with the water-fluorine-cerium systematics of basaltic glass. *Chem. Geol.* **522**, 283–294, doi:10.1016/j.chemgeo.2019.06.014 (2019).
37. Spadea, P. *et al.* Petrology of basic igneous rocks from the floor of the Sulu Sea. *Proceedings of the Ocean Drilling Program, Scientific Results* **124** (1991).
38. Zhang, G.-L. *et al.* Geochemical nature of sub-ridge mantle and opening dynamics of the South China. *Earth Planet. Sci. Lett.* **489**, 145–155, doi:10.1016/j.epsl.2018.02.040 (2018).
39. Hickey-Vargas, R. Origin of the Indian Ocean-type isotopic signature in basalts from Philippine Sea plate spreading centers: An assessment of local versus large-scale processes. *Journal of Geophysical Research-Solid Earth* **103**, 20963–20979, doi:10.1029/98jb02052 (1998).
40. Haase, K. *et al.* Magmatic evolution of a dying spreading axis: Evidence for the interaction of tectonics and mantle heterogeneity from the fossil Phoenix Ridge, Drake Passage. *Chem. Geol.* **280**, 115–125 (2011).
41. Pearce, J. *et al.* Composition and evolution of the Ancestral South Sandwich Arc: Implications for the flow of deep ocean water and mantle through the Drake Passage Gateway. *Global Planet. Change* **123**, 298–322 (2014).
42. Ryan, W. B. F. *et al.* Global Multi-Resolution Topography synthesis. *Geochemistry Geophysics Geosystems* **10**, doi:10.1029/2008gc002332 (2009).
43. Dixon, J. E., Stolper, E. & Delaney, J. R. Infrared spectroscopic measurements of CO 2 and H 2 O in Juan de Fuca Ridge basaltic glasses. *Earth Planet. Sci. Lett* **90**, 87–104 (1988).
44. Dixon, J. E., Stolper, E. M. & Holloway, J. R. An experimental study of water and carbon dioxide solubilities in mid ocean ridge basaltic liquids.1. Calibration and solubility models. *J. Petrol.* **36**, 1607–1631 (1995).
45. Cai, Y. *et al.* Distinctly different parental magmas for calc-alkaline plutons and tholeiitic lavas in the central and eastern Aleutian arc. *Earth Planet. Sci. Lett.* **431**, 119–126 (2015).
46. Todt, W., Cliff, R., Hanser, A. & Hofmann, A. Evaluation of a 202pb _ 205pb Double Spike for High-Precision Lead Isotope Analysis. *Earth processes: reading the isotopic code* **95**, 429 (1996).
47. Weis, D. *et al.* High-precision isotopic characterization of USGS reference materials by TIMS and MC-ICP-MS. *Geochemistry Geophysics Geosystems* **7**, doi:10.1029/2006gc001283 (2006).
48. Willbold, M. & Stracke, A. Formation of enriched mantle components by recycling of upper and lower continental crust. *Chem. Geol.* **276**, 188–197, doi:10.1016/j.chemgeo.2010.06.005 (2010).
49. Johnson, E. A. Water in nominally anhydrous crustal minerals: speciation, concentration, and geologic significance. *Rev. Mineral. Geochem.* **62**, 117–154 (2006).
50. Yang, X.-Z. *et al.* Water in minerals of the continental lithospheric mantle and overlying lower crust: a comparative study of peridotite and granulite xenoliths from the North China Craton. *Chem. Geol.* **256**, 33–45 (2008).
51. Kessel, R., Schmidt, M. W., Ulmer, P. & Pettke, T. Trace element signature of subduction-zone fluids, melts and supercritical liquids at 120–180 km depth. *Nature* **437**, 724–727,

doi:10.1038/nature03971 (2005).

Declarations

Acknowledgements This study was supported by the Strategic Priority Research Program (B) of Chinese Academy of Sciences, Grant No. XDB18000000, National Natural Science Foundation of China (41773025), and the Youth Innovation Promotion Association CAS (2020349) to A.Y.Y.

Author Contributions: A.Y.Y. and C.H.L. analyzed the data and conceived the study. A.Y.Y. compiled global MORB data, prepared the first draft of the manuscript, figures and tables, and with C.H.L. prepared subsequent drafts. Y.C. first identified the back arc signature in dredge 274. Y.C. and S.L.G. performed Sr, Nd and Pb isotopic analyses and P.M. collected H_2O data using Fourier Transform Infrared spectroscopy. Z.C. collected the major and trace element data using laser ablation inductively coupled plasma-mass spectrometry in the lab of C.H.L. All authors contributed to critical discussions and comments on the manuscript.

Supplementary Information is available for this paper.

Author Information: Correspondence and requests for materials should be addressed to A. Y. Y. (yangyang@gig.ac.cn) and C. H. Langmuir (langmuir@eps.harvard.edu). Reprints and permissions information is available at www.nature.com/reprints.

Figures

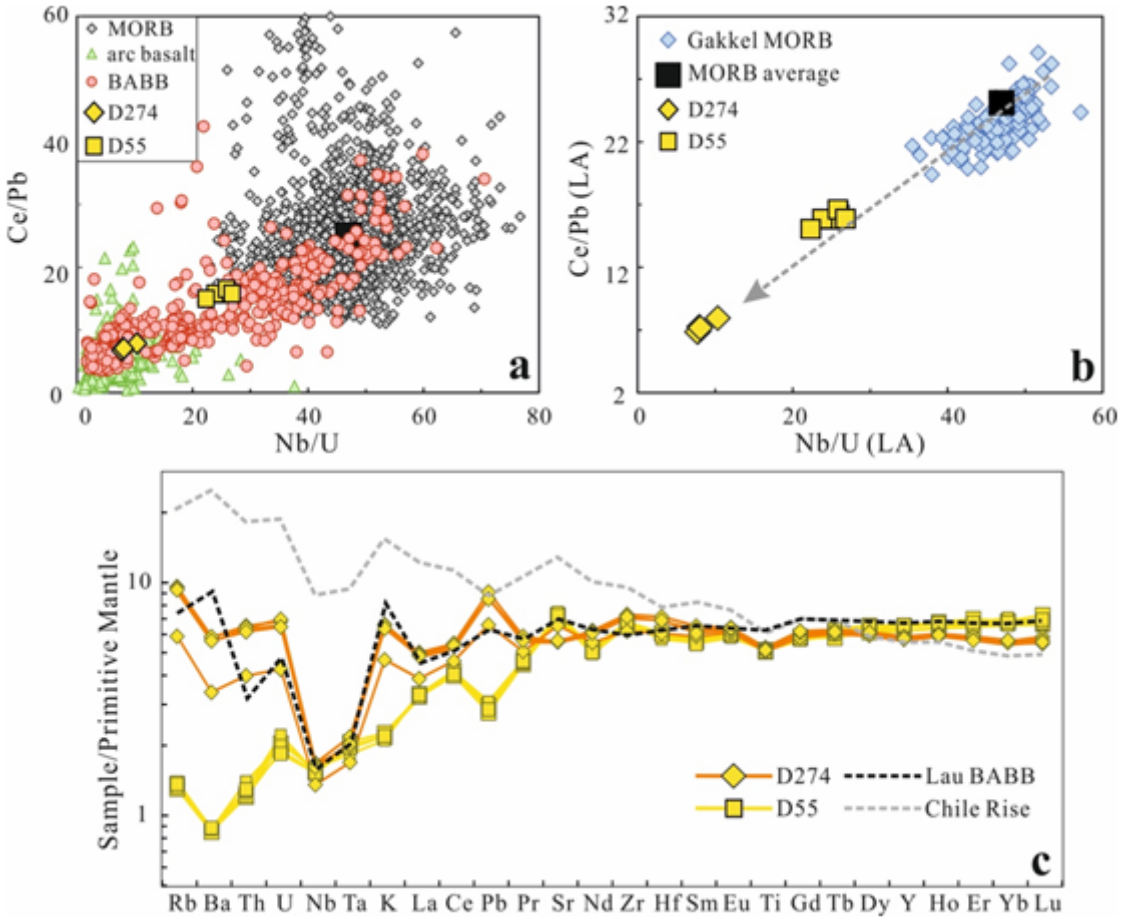

Figure 1

Trace element characteristics of Gakkel MORB. a. Ce/Pb vs. Nb/U plot for convergent-margin like MORB from Gakkel (Dredge 274&55). Global MORB and back-arc basin basalts (BABB) from Gale, et al. 12, as well as arc basalts from Turner and Langmuir6 are plotted for comparison. b. New high-quality laser ablation data of Gakkel MORB show positive Ce/Pb and Nb/U correlation. Gakkel MORB data were averaged per station (130 stations in total). Arrow shows the trend towards the influence of subduction component in Gakkel MORB. Average Nb/U and Ce/Pb ratios for MORB are from Hofmann, et al.4. c. Primitive mantle normalized trace element diagram for the convergent-margin like Gakkel MORB. Primitive mantle values are from McDonough and Sun34. MORB from Chile Ridge with convergent margin-like characteristics7 and average basalt compositions of Lau back-arc basin from 20-23°S calculated based on Gale, et al.12 are also plotted.

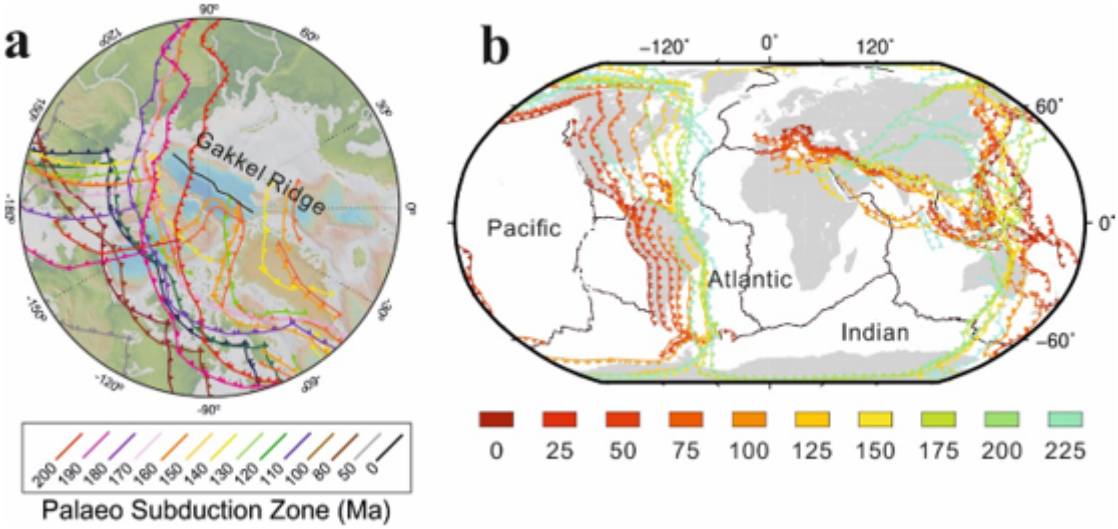

Figure 2

Reconstructed subduction locations for a) Arctic Ocean, and b) Indian and Atlantic Oceans, modified from Shephard et al.18 and Young et al.35. Note: The designations employed and the presentation of the material on this map do not imply the expression of any opinion whatsoever on the part of Research Square concerning the legal status of any country, territory, city or area or of its authorities, or concerning the delimitation of its frontiers or boundaries. This map has been provided by the authors.

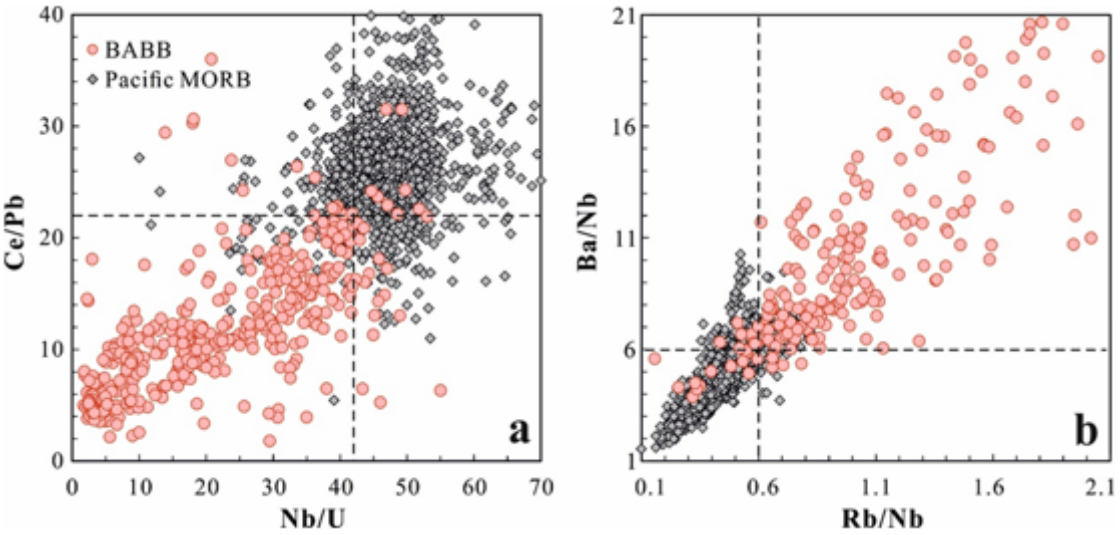

Figure 3

Plots of a) Ce/Pb vs. Nb/U and b) Ba/Nb vs. Rb/Nb for global BABB, as well as Pacific MORB. Note the clean separation of the two sets of data. The BABB samples can be well distinguished with Ba/Nb and Rb/Nb ratios higher than 6 and 0.6, and Ce/Pb and Nb/U ratios lower than 22 and 42, respectively. Global BABB data include volcanics from the Lau, Mariana Trough, Scotia and Manus back –arc basins. Data source can be found in the Supplementary Information.

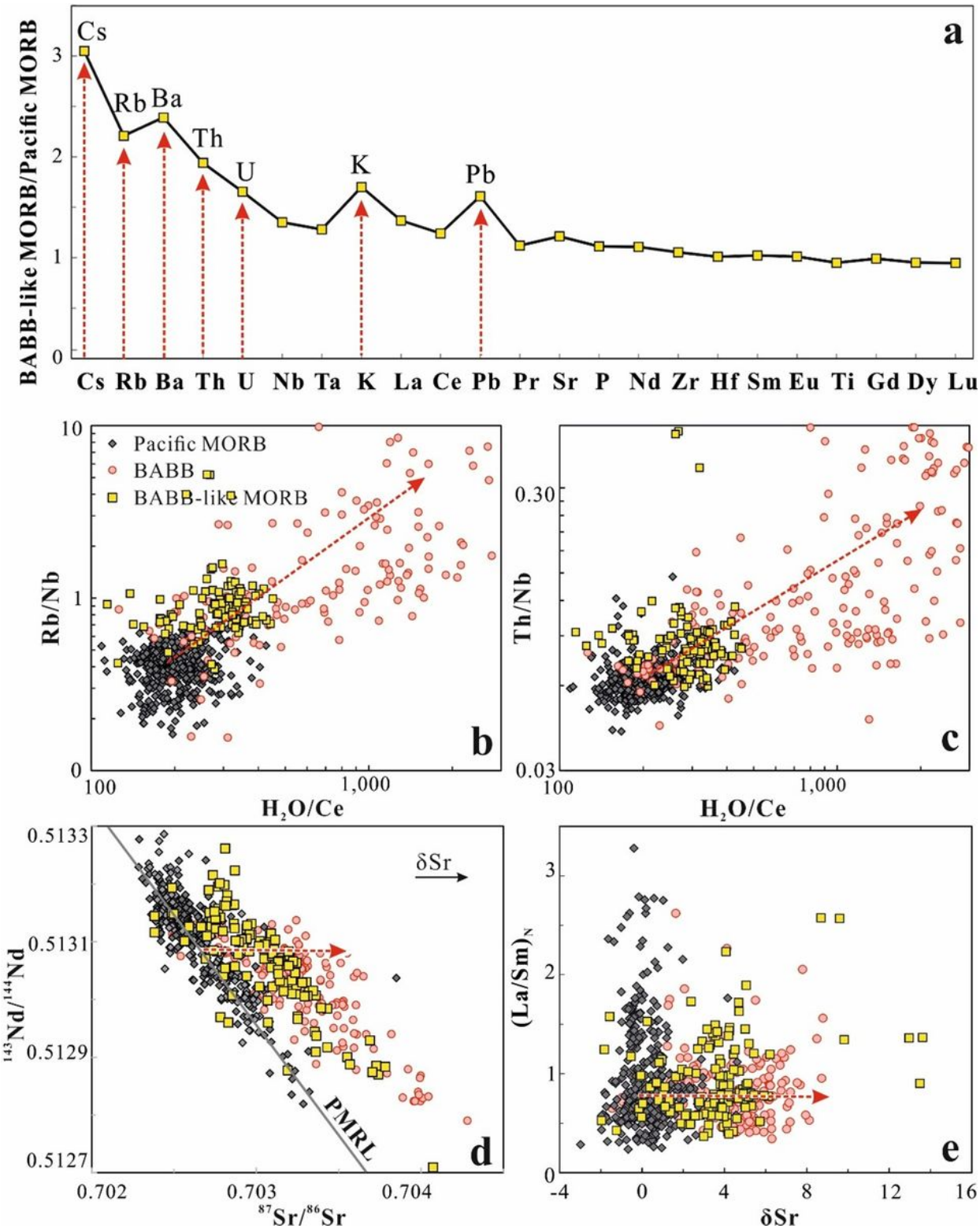

Figure 4

Chemical characteristics of BABB-like MORB relative to Pacific MORB and BABB. a) Enrichment factors of average BABB-like MORB relative to average Pacific MORB. BABB-like MORB show clear enrichments of Cs, Rb, Ba, Th, U, K and Pb relative to Pacific MORB. Average Pacific MORB compositions were calculated using Pacific MORB with MgO higher than 6 wt.%, so that the averages of the two groups have comparable MgO to minimize the effect of variable magma differentiation on the calculated results. b,c)

H2O/Ce vs. Rb/Nb, and Th/Nb, d) 87Sr/86Sr vs. 143Nd/144Nd, and e) δSr (Deviation of 87Sr/86Sr relative to the Pacific MORB reference line (PMRL), details of this line can be found in the Methods) vs. (La/Sm)N ratios for Pacific MORB, BABB and BABB-like MORB. The BABB-like MORB have higher H2O/Ce and shift to higher 87Sr/86Sr relative to 143Nd/144Nd ratios, but have comparable even slightly lower (La/Sm)N ratios than Pacific MORB. Red arrows indicate the direction for subduction input. Data source can be found in the Supplementary Information.

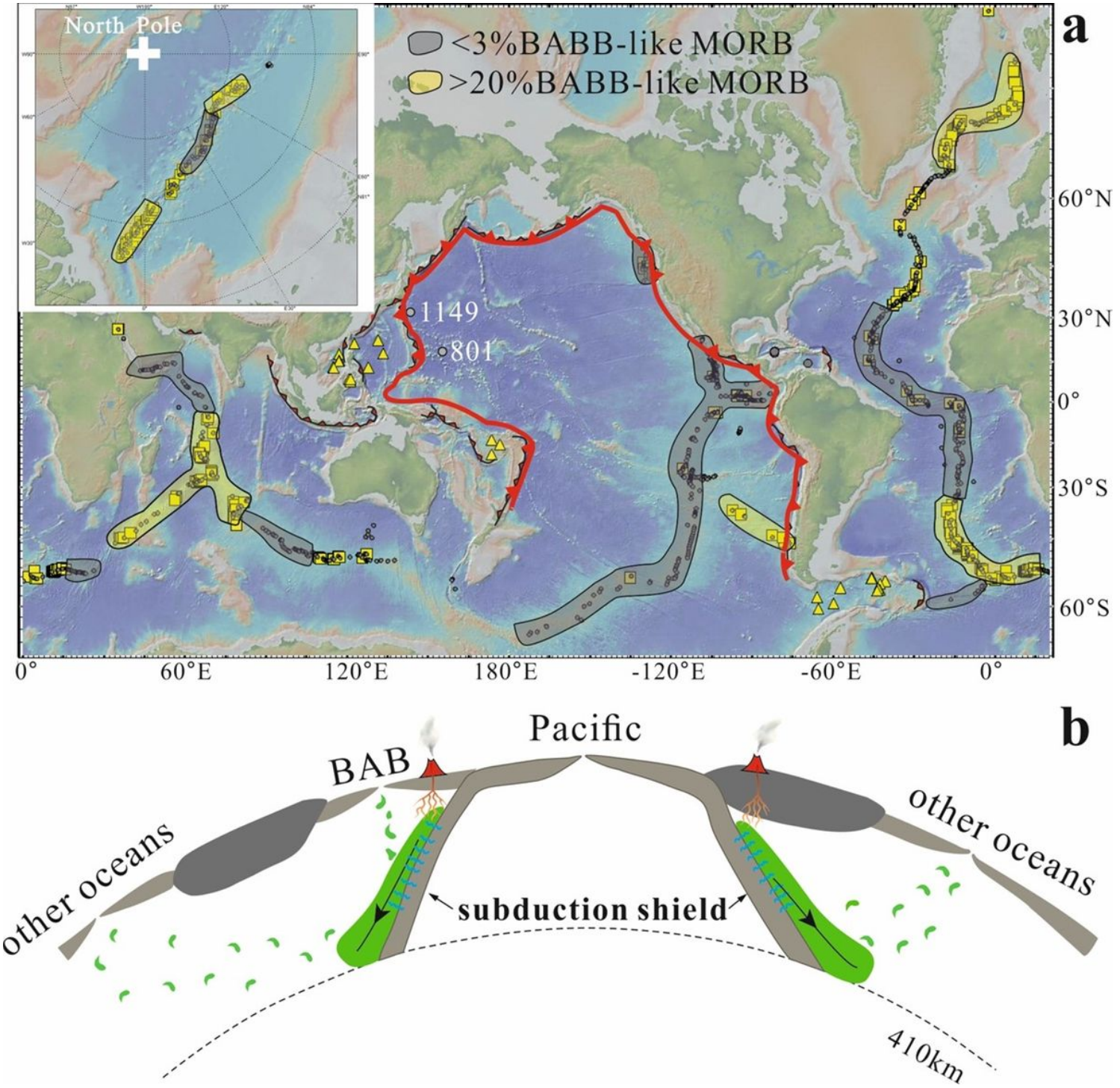

Figure 5

a) Distribution of global BABB-like MORB (yellow squares) and b) schematic model of the subduction shield. MORB samples which do not pass the BABB filter (grey dots) are also plotted. a. The majority of the global BABB-like MORB (yellow symbols) are distributed outside the Pacific subduction zones shown by the red lines. Yellow-shaded blobs denote ridge sections where >20% of MORB pass the BABB filter. Grey-shaded sections denote sections where <3% of MORB pass the filter. b. The circum-Pacific subduction zones form a subduction shield to prevent subduction contribution to Pacific MOR magmatism. Slab-derived fluids/melts (blue curves) would metasomatize the overlying mantle wedge (green shaded fields) right above the subducted slab. The metasomatized mantle would partially be dragged downwards by corner flow at mantle wedge and would not contribute to the arc volcanism. They would eventually mix into the convecting mantle to feed BAB and MOR magmatism. Old Pacific MORB glasses from drilled holes 1149 and 80128 (light grey dots) all have none ratios passing the BABB filter, and basalts from the Fiji36, Sulu Sea37, South China Sea38, Philippine Sea Plate23,39 and Drake Passage40,41 (yellow triangles) outside the Pacific subduction zones have BABB signatures, consistent with the subduction shield model. Global MORB data source can be found in the Supplementary Table S6. Bathymetry from GeoMapApp42. Note: The designations employed and the presentation of the material on this map do not imply the expression of any opinion whatsoever on the part of Research Square concerning the legal status of any country, territory, city or area or of its authorities, or concerning the delimitation of its frontiers or boundaries. This map has been provided by the authors.

Supplementary Files

This is a list of supplementary files associated with this preprint. Click to download.

- FalexandrayangXXXXXXXXXXXXGakkelnaturencommTable1.xlsx
- FalexandrayangXXXXXXXXXXXXGakkelnaturencommTable2.xlsx
- FalexandrayangXXXXXXXXXXXXGakkelnaturencommTable3.xlsx
- FalexandrayangXXXXXXXXXXXXGakkelnaturencommTable4.xlsx
- FalexandrayangXXXXXXXXXXXXGakkelnaturencommtable5.xlsx
- FalexandrayangXXXXXXXXXXXXGakkelnaturencommTable6.xlsx
- SupplementtextCHL122020.docx